Crack Propagation Analysis of Fatigue Due to External Corrosion on the Construction of the Ferris Wheel in Alun-Alun Kota Batu

Nur Subeki[1,*], Achmad Fauzan Hery Soegiharto[1], Andi Firkriyanto[1], Nadiaseptria Gidiazalia[2]

1   Department of Mechanical Engineering, Faculty of Engineering, University of Muhammadiyah Malang, Malang City, Indonesia
2   Department of Mechanical Engineering, Faculty of Engineering, Brawijaya University, Malang City, Indonesia

ARTICLE INFO	ABSTRACT
Article history: Received 10 July 2023 Received in revised form 12 September 2023 Accepted 28 September 2023 Available online 6 November 2023 *Keywords:* Ferris wheel; external corrosion; Stress Intensity Factor; crack; fatigue	Ferris wheel is the main structure of the form from steel structure; its strength is directly related to the safety of passengers. The risk of failure due to fatigue occurs in the support pipe rods due to defects with external corrosion and cracks due to stress concentrations. Inspection the crack indication at the defect point is carried out using the Liquid Penetrant Test method. Based on the inspection results, crack indications occurred at four defect location points. From the stress calculation, the value of the stress intensity factor is obtained at 4.52 Mpa√m, which still meets the fracture toughness value of 69.19 Mpa√m. The results of the calculation of fatigue analysis, namely in the form of fatigue life at the defect location at each crack point. The structure's life span in the most resounding crack is six years, according to the minimum allowable thickness of DNV RP F01, which is 70% of its thickness. Cracks will continue to spread to structural defects with corrosion. The risk of failure will continue to increase; even total loss of the structure will undoubtedly occur if it has passed its operational design period and will be faster with dynamic loads.

1. Introduction

The main structure of the Ferris wheel is a form of steel structure; its strength is directly related to the safety of passengers. In operation, steel construction will find various problems, such as problems of corrosion, crack, and fatigue. Corrosion and cracks are the main failure mechanism in structures. Corrosion arises due to the work of stress and corrosive media simultaneously, which can cause cracks [1]. The construction is easy to corrode by air pollution and moisture, contaminated with corrosive substances, and not coated with anti-corrosive [2]. So that the pipe rod installed in open locations has a significant chance of cracking, it is necessary to do mitigation for prevention. Corrosion is considered dangerous because it causes cracks. Crack propagation will be faster with the maximum loading of a corrosive environment.

Ferris wheel construction which is tilted due to the shifting ground contours, will result in friction between the rim and the supporting rod of the Ferris wheel. The problem will cause scratches/defects

---

that are deep enough on the support pipe rod and will continue to increase as the rim rotates. The structure's slope affects the increase in bending loads on specific constructions, causing them to break due to overload [3, 4] . Scratches on the pipe are the beginning of the crack. Rift will propagate faster due to dynamic load and combined with corrosion [5, 6] . The presence of external corrosion exacerbates the defects in the structure due to the electrochemical interaction of the material with the environment. These corroded defects can trigger cracks in the pipe and allow the failure of a structure. The leading cause is external and internal corrosion [7]. Structures deformed by corrosion during operation have a significant chance of *cracking* due to dynamic loads [8]. The existence of corrosion, followed by the existence of pressure on the supporting pipe rod, is called Stress Corrosion Cracking (SCC) [9, 10]. Structures that experience degradation or thinning of the corroded pipe wall surface will experience a decrease in strength. Defects will grow cracks that are getting longer and affect the material's structural strength [11] . So, it is necessary to analyze the crack propagation of the supporting pipe rod at the point of defect. It aims to be able to determine the rate of crack propagation that occurs in the defective part.

Based on this research, using A36 material with material specifications maximum yield stress of 167 MPa, maximum tensile stress of 306 MPa, and elongation of 23%. Based on the chemical composition of C and Mn, the parent metal A36 is carbon steel with a weight % of Mn of 0.4711. In contrast to the parent metal, the % C is 0.1246%. Surian *et al.,* (2010). Changes in the weight of carbon (C) and manganese (Mn) elements in metals can increase welding joints' tensile strength and toughness. Mn content in more significant metals includes increasing strength and hardness, meeting the critical cooling rate, and binding sulfur to minimize the formation of iron sulfide (FeS), which causes heat brittle.

Based on the problems in constructing the Ferris wheel, the focus will be on developing a probabilistic method. It aims to predict the probability of failure and fatigue life of supporting pipe stems due to corroded defects. Macrographic crack inspection with the Non-Destructive Test uses the Dye Penetrant Test method at the rusty defect point. Then, an analysis of fatigue crack propagation is carried out to predict the probability of failure and fatigue life in an integrated manner. So that further problems can be identified that must be watched out for and prevented, and can provide more effective and efficient inspection ideas.

2. Methodology

The method used in this research is a field study and experimental methods to obtain the necessary data. Field studies were conducted to identify problems and complete the data in this study. Experimental research was conducted to find out and correctly test the hypothesis of this research. The literature study used comes from related references, books, and journals so that it can add the necessary information. This research begins by identifying the problems that occur. Data collection is in the form of non-inspection data, Destructive tests, and operational data. This study uses NDT and liquid penetrant testing methods to detect crack indications. The inspection results that have been carried out aim to obtain the relationship between each parameter and variable used for calculations. Calculation This includes calculating the Stress Intensity Factor (SIF), calculating the rate of crack propagation, and analysis of the fatigue life of the structure. The results of this calculation are used to predict the probability of failure and fatigue life of the Ferris wheel supporting pipe stem due to corroded defects.

2.1 Inspection Equipment

The equipment used in this inspection includes liquids remover, red penetrant, and developer. The inspection medium is the Ferris wheel central support pipe rod.

2.2 Research Procedure

Inspection is done directly on constructing a Ferris wheel in *Alun-alun Kota Batu* on the part of the Ferris wheel support pipe that has defects/scratches. At that point, two semi-elliptical cracks (Figure 1) with external corrosion attacked. Further liquid penetrant testing was carried out to identify the presence of cracks on the surface of the defect. The discontinuity of crack detection is indicated by the presence of red spots of penetrant that appear [12]. The penetrant test used is the visible type of penetrant liquid with the removable solvent method [13]. Penetrant testing of liquids is carried out by ASME Section V standards [14].

After the Non-Destructive Testing (liquid penetrant) is completed, calculate the stress on the Ferris wheel supporting pipe stem due to internal and external pressure. The following is the formulation used in calculations based on ASME B 31.3 [15-17]:

$$Hs = \frac{(Pi - Pe)D}{2t} = (\text{Mpa}) \tag{1}$$

Next, calculate the value of the Stress Intensity Factor (SIF or KI $_)$ in the case of cracks that occur on the surface of the pipe using the following equation formulation [5]:

$$K_I = Hs \sqrt{\pi \frac{a}{Q}} = (\text{Mpa}\sqrt{m}) \tag{2}$$

Before calculating the SIF value, it must determine the defect parameters according to the conditions at 4 points where defects and cracks occur.
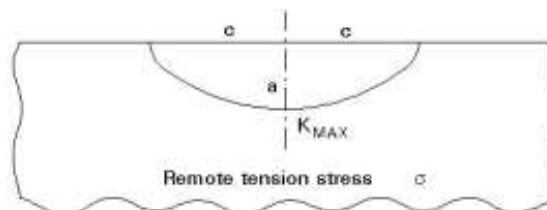

Fig. 1. Semi-elliptical Crack [5]

The Q value is obtained from the flaw shape parameter Q graph, as shown in Figure 2, by connecting the values $\frac{a}{2c}$ and $\frac{\sigma}{\sigma ys}$ [5].
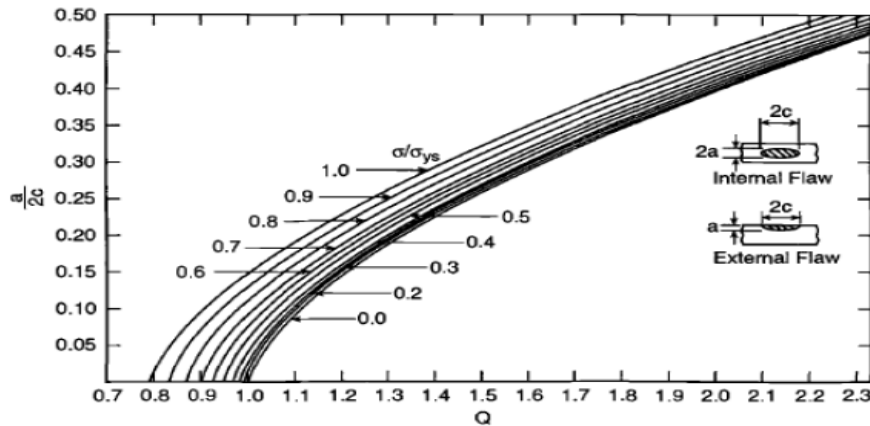
Fig. 2. Crack defect parameters in surface crack conditions

Based on the Paris-Erdogan law, the ΔK value is obtained from the difference between the K value at maximum loading and the K value at minimum loading. SIF ranges between maximum and minimum loading [5, 18].

$$\Delta K_I = K_{Imax} - K_{Imax} = (Mpa\sqrt{m}) \tag{3}$$

Crack propagation began to occur. Crack propagation speed can be calculated using the Paris-Erdogan law, which describes the relationship between fatigue crack propagation and stress intensity factor. [5]:

$$da/dN = C (\Delta K)^m = (m/cycle) \tag{4}$$

Calculate the fatigue life of deformed and corroded support pipe stems with crack indications by incrementing the corrosion depth until it reaches the depth permitted by DNV RP F01 [19].

Propagation rate of fatigue crack (dα/dN) versus intensity of strength (ΔK) and their trend line that As welded A 36 have C is $2.161 E^{-11} - 6.171E^{-11}$ and n is $4.112 - 4.127$ Failure occurs when $K_I = K_{Ic}$. In this case, K_I is the driving force for fracture, and KIc is a measure of material resistance. As with Gc, the property of similitude should apply to KIc. That is, KIc is assumed to be a size-independent material property. (Subeki 2017, subki 2017). Figure 3 shows the location pipelines.

Fig. 3. Location pipelines

Form construction Ferris the high, rotating wheel, is also very prone to burden dynamic. It can trigger happening propagation cracked fatigue due to external corrosion cracks, as in Figure 4.

Fig. 4. Friction between the rim and the support pipe that causes happening scratches/flaws

Figure 5 forms from defects that occur consequence tilt of the Ferris wheel so that the rim and rod pipe support experience friction. It resulted from the formation of a disabled semi-elliptical. Especially aggravated with exists suitable corrosion with indication exists propagation cracks that occur.
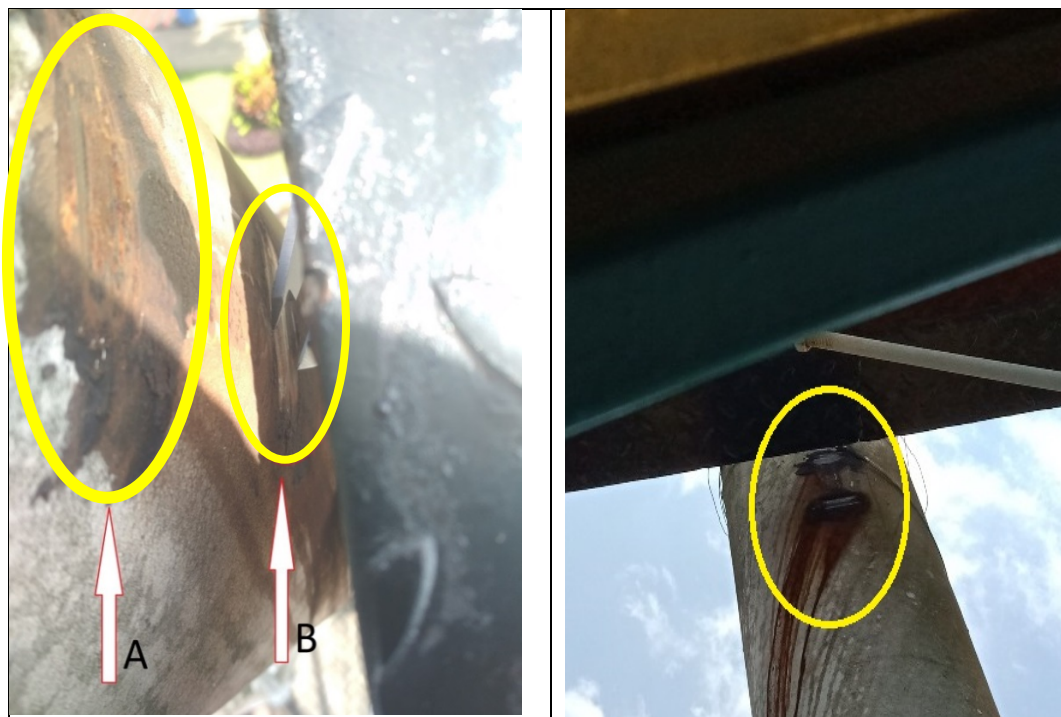

Fig. 5. Locations A and B of scratches/defects and corrosion on steel pipes buffer Ferris wheel consequence friction with rims

3. Results

Ferris wheel construction that has problems and has gone through inspection will be processed into the testing phase. Non Destructive Test with Liquid Penetrant Test method on corroded defect points. After that, a probabilistic method was developed to predict the probability of failure and the fatigue life of the Ferris wheel supporting pipe stem due to corroded defects. Then calculate, the value of the Stress Intensity Factor and analysis of fatigue crack propagation to predict the probability of failure and fatigue life in an integrated manner. The results of the testing and analysis of the calculations that have been carried out will then be discussed as follows:

3.1 Liquid Penetrant Test Results

They did Liquid Penetrant Test because it can detect open macro cracks from the material's surface. This test aims to detect the presence of cracks at the point of defect. The following is a macrographic image and table of Liquid Penetrant Test results on defects A and B at the inspection point.

From inspection, The Liquid Penetrant Test and macrographic results above obtained data from the inspection point, as shown in Figure 6 and Table 1. From the inspection results Non the Destructive Test with the Liquid Penetrant Test method at location points, the defect is visible with indications of cracks at 4 points at defect locations A and B. The most extended crack indication occurs at point 3 along 8.3 mm. Meanwhile, the shortest c rack happens at point 4 along 5.5 mm. With the above test, it was obtained that the initial crack sides were visible, then the crack propagation was indicated by the beach mark. An indication of crack propagation occurs, namely the presence of beach marks around the location of the crack indication [9, 20].

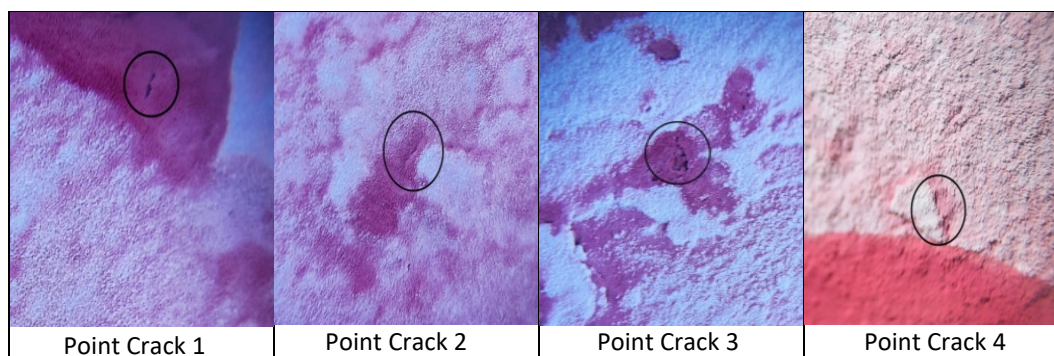| Point Crack 1 | Point Crack 2 | Point Crack 3 | Point Crack 4 |

Fig. 6. Macrographic results from penetrant testing at the defect inspection point

Table 1
Inspection Data Liquid Penetrant Tests

Crack Point	Crack Location	Crack Length (mm)	Presence of Cracks
1	A handicap	6,4	Crack
2	A handicap	7,5	Crack
3	B defects	8,3	Crack
4	B defects	5,5	Crack

3.2 Results of Calculation of Stress Intensity Factor (SIF or K_1)

After reviewing the results of the *crack data,* proceed to calculate the SIF value by determining the defect parameters according to the crack conditions that occur at 4 points. The following are the defect parameters at each point as described in the Table 2 and Table 3 below:

Table 2
The price of Q with a maximum loading of Hs/Sys = 0.3

Crack Point	Crack depth (a)(m)	Crack Length (2c)(m)	a/2c	Q
1	0.99×10^{-3}	0.0064	0.15	1.19
2	1.28×10^{-3}	0.0075	0.17	1.21
3	1.35×10^{-3}	0.0083	0.16	1.20
4	0.75×10^{-3}	0.0055	0.13	1.12

Table 3
The price of Q with a minimum loading of Hs/Sys = 0.2

Crack Point	Crack depth (a)(m)	Crack Length (2c)(m)	a/2c	Q
1	0.99×10^{-3}	0.0064	0.15	1.20
2	1.28×10^{-3}	0.0075	0.17	1.22
3	1.35×10^{-3}	0.0083	0.16	1.21
4	0.75×10^{-3}	0.0055	0.13	1.13

Table 2 and Table 3 show that a different Q value is obtained for each crack variation at the maximum and minimum loading. The Q price received is the highest at the maximum loading of 1.21 and the smallest at 1.12. At minimum loading, the most significant Q value is 1.22, and the smallest is 1.13. After the Q value is obtained, the SIF value calculation results at each crack point with maximum and minimum loading can be seen. The following results in calculating the SIF value are shown in Table 4 and Table 5.

Table 4
SIF calculation results with maximum loading

Crack Point	Mpa√m
1	3.88
2	4.36
3	4.52
4	3.48

Table 5
SIF calculation results with minimum loading

Crack Point	Mpa√m
1	2.06
2	2.32
3	2.40
4	1.85

The SIF calculation shows that the largest SIF is 4.52 Mpa√m at maximum loading, and the largest SIF at minimum loading is 2.40 Mpa√m. The SIF value will decrease in proportion to the more minor the crack length. On the other hand, it continues to increase crack variation as the size of the crack depth increases and the length of the crack grows. At this stage, the SIF value still meets Fracture Toughness (KIC), where the Fracture Toughness (KIC) for ASTM A36 material is 69.19 Mpa√m. SIF values that exceed fracture toughness will cause failure [21].

3.3 Calculation Results of Range Stress Intensity Factor (ΔK)

Based on the Paris-Erdogan law, the ΔK value is obtained from the difference between the K value at maximum loading and the K value at minimum loading. The following results are obtained from the SIF range between maximum and minimum loading.

Based on the results of the description presented In Table 6, the value of the Range Stress Intensity Factor (ΔK) is greatest shown at crack point 3, equal to 2.12 Mpa√m. This most significant value is partly obtained with the longest and deepest crack among the other crack points. The larger the crack size, length, and depth, the greater the ΔK value obtained. Likewise, the magnitude of the tensile axial load that affects the opening mode the greater the value of the Range Stress Intensity Factor [22].

Table 6
Range Stress Intensity Factor (ΔK)

Crack Point	K_I (Mpa√m)		ΔK_I (Mpa√m)
	Maximum	Minimum	
1	3.88	2.06	1.82
2	4.36	2.32	2.04
3	4.52	2.40	2.12
4	3.48	1.85	1.63

3.4 Calculation Results of Crack Propagation Rate

The results obtained from calculating the crack propagation rate at each crack point due to defects that occur with compounded corrosion are shown in Table 7 according to the da/dN calculation as follows:

Table 7
Crack Propagation Rate

Crack Number	a_0 (mm)	KI (Mpa√m)		ΔKI (Mpa√m)	da/dN (m/cycle)
		Kmax	Kmin		
1	0.99	3.88	2.06	1.82	2.17E-09
2	1.28	4.36	2.32	2.04	3.06E-09
3	1.35	4.52	2,4	2.12	3.43E-09
4	0.75	3.48	1.85	1.63	1.56E-09

Based on the table above, the crack propagation rate at each point is known. The crack propagation rate expressed by da/dN experienced the most critical propagation speed at crack 3, 3.43E-09 m/cycle. At this point, it becomes the weakest area and will develop as the loading cycle progresses. Metals subjected to repeated stresses and loads will break down under stress with specific processes leading to fracture and failure. This failure is marked with a defect/crack [6].

3.5 Fatigue Age Calculation Results

The calculation data for the fatigue life of the Ferris wheel structure is carried out by incrementing the corrosion depth until it reaches the depth permitted by DNV RP F01 [19]. It discusses the maximum allowable criteria due to defects that occur with corrosion. The critical crack propagation rate and fatigue life at each crack point can be seen in the following Table 8 to 11:

Table 8
Fatigue life at crack point 1 to the allowable thickness

da/dN (m/cycle)	Cycles/Year	Year	AF(m)
2.17E-09	1000	1	0.79×10^{-3}
2.17E-09	1000	2	1.58×10^{-3}
2.17E-09	1000	3	2.38×10^{-3}
2.17E-09	1000	4	3.17×10^{-3}
2.17E-09	1000	5	4×10^{-3}
2.17E-09	1000	6	4.75×10^{-3}
2.17E-09	1000	7	5.55×10^{-3}
2.17E-09	1000	8	6.34×10^{-3}
2.17E-09	1000	9	7.13×10^{-3}

Table 9
Fatigue life at crack point 2 to the allowable thickness

da/dN (m/cycle)	Cycles/Year	Year	AF(m)
3.06E-09	1000	1	1.16×10^{-3}
3.06E-09	1000	2	2.23×10^{-3}
3.06E-09	1000	3	3.35×10^{-3}
3.06E-09	1000	4	4.46×10^{-3}
3.06E-09	1000	5	5.58×10^{-3}
3.06E-09	1000	6	6.69×10^{-3}

Table 10
Fatigue life at crack point 3 to the allowable thickness

da/dN (m/cycle)	Cycles/Year	Year	AF(m)
3.43E-09	1000	1	1.25×10^{-3}
3.43E-09	1000	2	2.5×10^{-3}
3.43E-09	1000	3	3.76×10^{-3}
3.43E-09	1000	4	5.01×10^{-3}
3.43E-09	1000	5	6.26×10^{-3}
3.43E-09	1000	6	7.51×10^{-3}

Table 11
Fatigue life at crack point 4 to the allowable thickness

da/dN (m/cycle)	Cycles/Year	Year	AF(m)
1.56E-09	1000	1	0.57×10^{-3}
1.56E-09	1000	2	1.14×10^{-3}
1.56E-09	1000	3	1.71×10^{-3}
1.56E-09	1000	4	2.28×10^{-3}
1.56E-09	1000	5	2.85×10^{-3}
1.56E-09	1000	6	3.41×10^{-3}
1.56E-09	1000	7	3.98×10^{-3}
1.56E-09	1000	8	4.55×10^{-3}
1.56E-09	1000	9	5.12×10^{-3}
1.56E-09	1000	10	5.69×10^{-3}
1.56E-09	1000	11	6.26×10^{-3}
1.56E-09	1000	12	6.83×10^{-3}

From the results obtained in Table 10, the crack propagates very quickly at crack point 3 with a critical crack depth of 0.0075 meters which occurred in the 6th year from the start of the initial crack. Reference used according to DNV RP F101 criteria [19]. The assumptions used are the number of cycles /year, which is 1000 cycles, and the allowable depth of defects, up to a depth of 0.0065 meters

or up to 70% pipe thickness. When *the crack* has passed the permissible tolerance, the material must be replaced immediately to anticipate failure that will occur. Cracks that start at critical locations can cause the failure of the structure if its presence is not known. Moreover, it is exacerbated by the fact of corrosion [23].

Table 12 shows that the life of the shortest Ferris wheel support pipe stem from the 4 points of defects/ cracks that are corrupted, reaching 70% of the pipe thickness, is six years, and the most extended life is 12 years. This shortest life is not much different from the maximum design life determined at the beginning of planning, namely 15 years. Based on the behavior of the fatigue life in the table below, it is clear that the fatigue strength and fatigue limit at each crack point is very different. This is due to the effect of stress concentration on the defects A and B that occur. The defects will deepen due to the rim and support rods rubbing each time the Ferris wheel operates at full load. This is due to the steel construction structure, which has been tilted due to the soil shifting. The position of the structure dramatically determines the performance of steel structures. Construction shifts can cause an increase in loads on certain sides and will also interfere with components that experience rotation [24].

Table 12
Calculation of Fatigue Life at Each Crack Point

Crack Number	Pipe Thickness(mm)	Residual Thickness(m)	Age (years)
1	12.76	5.63×10^{-3}	9
2	12.76	6.06×10^{-3}	6
3	12.76	5.24×10^{-3}	6
4	12.76	5.93×10^{-3}	12

When the loading is too large, it can produce cracks due to fatigue, and cracks are initiated from the maximum stress. If the crack spreads to the defective part of the structure, the risk of failure will continue to increase. Total failure of the structure is certain to occur. Therefore, if the structure has passed its operational design period, it must be replaced immediately. Mainly to be considered is fatigue and pipe breakage in the defective section due to friction of the rim and support rod of the Ferris wheel. Pantazopoulos states that the age of construction with dynamic loads is seven years, after which it is prone to fracture [25]. He explained that in steel construction, structures fail due to dynamic loads.

In this research, a die penetrant test (Non-destruction test) was carried out on the surface of various important part locations on the Ferris Wheel. At various part locations, it was observed that cracks appeared along with corrosion. Over time, crack-induced corrosion accumulates on the surface and begins to press against the steel surface (concrete cover). Corrosion has a volume between 4 and 6 times the initial volume of the steel. The additional volume due to corrosion will cause compression and tension in the concrete. If the tensile stress exceeds the tensile strength of the steel, a crack will occur. Tracing the production process found that the anticorrosive treatment only relied on painting and no other anticorrosive treatment. This study recommends the importance of adequate anticorrosive treatment in the construction process of the Ferris Wheel.

4. Conclusions

From the results of the Non-Destructive Test with the Liquid method, Penetrant Test at the point where there is a defect, it is clear that there are indications of cracks at 4 points at the location of defects A and B. Crack indications that occur at points 1 6.4 mm long, point 2 7.5 mm long, point 3 8.3 long mm, and point 4 5.5 mm long. The most significant Stress Intensity Factor (SIF) value with a

known maximum loading of 4.52 Mpa√m. This SIF value is still too far from fulfilling fracture toughness, equal to 69.19 Mpa√m, a critical SIF value. So that the pipe stem still meets the design criteria. If viewed from the point of the most resounding crack, the result is obtained from the remaining fatigue life of 6 years. This fatigue life refers to the minimum allowable pipe thickness tolerance of DNV RP F101, which is 70% of the pipe thickness. So the pipe supporting the Ferris wheel must be mitigated immediately. This aims to replace the entire structure if it has passed its operational design period. This research recommends the importance of adequate anticorrosive treatment in the construction process of the Ferris Wheel.

Acknowledgement

References

[1]   Moss, Tyler, Wenjun Kuang, and Gary S. Was. "Stress corrosion crack initiation in Alloy 690 in high temperature water." *Current Opinion in Solid State and Materials Science* 22, no. 1 (2018): 16-25. https://doi.org/10.1016/j.cossms.2018.02.001

[2]   Dai, Hailong, Shouwen Shi, Can Guo, and Xu Chen. "Pits formation and stress corrosion cracking behavior of Q345R in hydrofluoric acid." *Corrosion Science* 166 (2020): 108443. https://doi.org/10.1016/j.corsci.2020.108443

[3]   N. Perez, *FRACTURE MECHANICS.* New York, Boston, Dordrecht, London, Moscow: Kluwer Academic, UMM Central Library, 2004.

[4]   Tammas-Williams, S., Philip J. Withers, I. Todd, and P. B. Prangnell. "The influence of porosity on fatigue crack initiation in additively manufactured titanium components." *Scientific reports* 7, no. 1 (2017): 7308. https://doi.org/10.1038/s41598-017-06504-5

[5]   J. Barsom and S. Rolfe, *Fracture and Fatigue Control in Structures: Applications of Fracture Mechanics, Third Edition.* UMM Central Library, 1999. https://doi.org/10.1520/MNL41-3RD-EB

[6]   Xue, Songling, Ruili Shen, Wei Chen, and Rusong Miao. "Corrosion fatigue failure analysis and service life prediction of high strength steel wire." *Engineering Failure Analysis* 110 (2020): 104440. https://doi.org/10.1016/j.engfailanal.2020.104440

[7]   Trethewey, K. R., and J. Chamberlein. "Corrosion, for Science and Engineering Students." *Alex TKW, Grame dia Pustaka Utama, Jakarta* (1991).

[8]   Subeki, Nur, Jamasri Jamasri, M. Noer Ilman, and Priyo Tri Iswanto. "The Influence of Preheat on Distortion and Fatigue Crack Propagation Rate of FCAW Weld in A 36 Steel Structure." *Applied Mechanics and Materials* 842 (2016): 83-91. https://doi.org/10.4028/www.scientific.net/AMM.842.83

[9]   Dieter and George E, *Mechanical metallurgy vol 1 / George E. Dieter; subtitles: Sriati Djaprie*, vol. 1996. UMM Central Library, 1996.

[10]   Rajasekaran, R., A. K. Lakshminarayanan, R. Damodaram, and V. Balasubramanian. "Stress corrosion cracking failure of friction stir welded nuclear grade austenitic stainless steel." *Engineering Failure Analysis* 120 (2021): 105012. https://doi.org/10.1016/j.engfailanal.2020.105012

[11]   Ilman, M. N., and R. A. Barizy. "Failure analysis and fatigue performance evaluation of a failed connecting rod of reciprocating air compressor." *Engineering Failure Analysis* 56 (2015): 142-149. https://doi.org/10.1016/j.engfailanal.2015.03.010

[12]   ASM International, "ASM Metals Handbook Vol.17, Non-destructive Evaluation and Quality Control," *Technology*, 1997.

[13]   B. Hull, and V. John, " Liquid Penetrant Inspection, "in *Non-Destructive Testing*, 1988. https://doi.org/10.1007/978-1-349-85982-5

[14]   ASME SECTION V, *Non-destructive Examination.* 10016-5990 USA: The American Society of Mechanical Engineers, 2013.

[15]   THE AMERICAN SOCIETY OF MECHANICAL ENGINEERS, "ASME B31.3 Process Piping - Code for Pressure Piping," *Am. Soc. Mech. Eng.* , vol. 76, no. 8, pp. 95–108, 2012.

[16]   Meteorology, Climatology, and Geophysics Agency, "DATA ONLINE - DATA CENTER BASE BMKG," *BMKG.* Available: https://dataonline.bmkg.go.id/home. [Accessed: 07-Mar-2021].

[17]   SNI 1723, "Minimum load for the design of buildings and other structures of the National Standardization Agency," *Nas Standard. Indonesia. 1723*, 2013.

[18]   Dimas Wahyu Arie Chandra, "Analysis of Pipe Reliability Against Fatigue Due to Pitting Corrosion," Final Project,

Department of Marine Engineering FTK ITS, 2016.

[19] (DNV) Det Norske Veritas, "Fatigue Design of Offshore Steel Structures," *Recomm. Pract. DNV-RP-C203*, p. 126, 2010.

[20] Basuki, Eddy A., Ikhsan Septiansyah, Akhmad A. Korda, and Hilman Hasyim. "Effects of Welded Microstructure on Fracture Toughness and Crack Propagation Behavior of API 5L-X65 Pipe." *International Journal of Engineering & Technology IJET-IJENS* 17, no. 05 (2017).

[21] IS Putra, "ITB Scientific Meeting Hall: The Use of Crack Mechanics in the Stress Analysis of Defective Aircraft Structures," Assembly of Professors I TB, 2010.

[22] A. Puspaningtyas, "Parametric Study of Stress Intensity Factor (SIF) on Fracture Mechanics-Based Multiplanar Tubular Joints," Final Project, Department of Marine Engineering FTK ITS, 2016.

[23] Maliwemu, E. U. K., V. Malau, P. T. Iswanto, I. Kambali, and T. Sujitno. "Corrosion fatigue crack propagation of AISI 316L by nitrogen ion implantation in simulated body fluid." *Metalurgija* 60, no. 1-2 (2021): 43-46.

[24] Martelo, D. F., A. Mateo, and M. D. Chapetti. "Crack closure and fatigue crack growth near threshold of a metastable austenitic stainless steel." *International Journal of Fatigue* 77 (2015): 64-77. https://doi.org/10.1016/j.ijfatigue.2015.02.016

[25] Pantazopoulos, George, Athanasios Vazdirvanidis, Andreas Rikos, and Anagnostis Toulfatzis. "Analysis of abnormal fatigue failure of forklift forks." *Case Studies in Engineering Failure Analysis* 2, no. 1 (2014): 9-14. https://doi.org/10.1016/j.csefa.2013.12.005